Exploring the effects of crop growth differences on radar vegetation index response and crop height estimation using dynamic monitoring model

Bo Wang [1], Yu Liu [1], Qinghong Sheng [1], Jun Li [1], Shuwei Wang [2], Yunfeng Qiao [3], Honglin He [4]

[1] College of Astronautics, Nanjing University of Aeronautics and Astronautics, Nanjing, China – (wangbo_nuaa, lyu, qhsheng, junlii) @nuaa.edu.cn
[2] Changshu National Agro-Ecosystem Observation and Research Station, Institute of Soil Science, Chinese Academy of Sciences, Nanjing, China - swwang@issas.ac.cn
[3] Institute of Geographic Sciences and Resources, Chinese Academy of Sciences, Beijing, China – qiaoyf@igsnrr.ac.cn
[4] Key Laboratory of Ecosystem Network Observation and Modeling, Institute of Geographic Sciences and Natural Resources Research, Chinese Academy of Sciences, Beijing, China – hehl@igsnrr.ac.cn

Keywords: Crop height, Dynamic monitoring, Growth differences, Multi-temporal Sentinel-1, Radar vegetation index.

Abstract

Synthetic aperture radar (SAR) has emerged as a promising technology for monitoring crop plant height due to its ability to capture the geometric properties of crops. Radar vegetation index (RVI) has been extensively utilized for qualitative and quantitative remote sensing monitoring of vegetation growth dynamics. However, the combination of crop, growing environment, and temporal dynamics makes crop monitoring data a complex task. Despite the relatively simple underlying mechanisms of this phenomenon, there is still a need for more research to identify specific vegetation structures that correspond to changes in the response of vegetation indices. Building upon this premise, this study utilized a dynamic monitoring model to conduct dynamic monitoring of plant height for three common crops: rice, wheat, and maize. The findings revealed that (1) models developed for specific spatial and temporal scales of particular crop varieties may not accurately predict crop growth in different regions or with different varieties in a timely manner, due to growth variations; (2) these models maintain accuracy over a range of plant heights, such as rice at around 70cm, wheat at around 50cm, and maize at around 150cm; (3) among the three crops, planting density was identified as the main factor influencing the differences in RVI response. This research contributes to our comprehension of the dynamic response of RVI to different growth conditions in crops, and offers valuable insights and references for agricultural monitoring.

1. Introduction

Plant height (PH) is a crucial indicator that dynamically measures the health and overall growth condition of crops. It reflects the ability of crops to vertically extend and provides a reliable basis for assessing crop growth, guiding farm management, and predicting grain yield (Chang et al., 2017; Erten et al., 2016). Traditional methods of measuring plant height primarily rely on field surveys, which are resource-intensive and time-consuming. However, satellite remote sensing has emerged as the primary method for obtaining crop information at local, regional, and global scales by revealing the spatial and temporal dimensions of crop growth status and production (Weiss et al., 2020; Wu et al., 2023). Synthetic Aperture Radar (SAR) stands out among different types of remote sensing payloads due to its unparalleled advantages in monitoring crops in regions affected by weather conditions. Moreover, SAR exhibits excellent sensitivity to differences in crop canopy structure, making it a proven method for measuring plant height (McNairn and Shang, 2016; Pang et al., 2021; Steele-Dunne et al., 2017).

The backscattering coefficient is a measure of how well a target scatters radar signals in the direction of radar incidence. Many researchers have studied the use of backscatter coefficients to develop vegetation indices that can improve vegetation signals. Several studies have investigated different vegetation indices derived from polarimetric synthetic aperture radar (SAR) data. Blaes et al. (2006) examined the sensitivity of the polarization ratio index (PRI) to plant growth. They found that PRI had a stronger correlation with fresh grain biomass and the normalized difference vegetation index (NDVI) compared to the single-channel backscattering response. Kim and Van Zyl (2009) proposed the full-pol radar vegetation index (RVI), which was later modified for Sentinel-1 dual-pol data (VV and VH) as $4\sigma_{vh}^0/(\sigma_{vv}^0 + \sigma_{vh}^0)$. This index focuses on the contribution of volume scattering, as indicated by the cross-polarized response (Nasirzadehdizaji et al., 2019). Periasamy (2018) introduced the dual-polarization SAR vegetation index (DPSVI) by studying the physical scattering behavior of multiple targets in the polarimetric and cross-polarization channels of Sentinel-1. DPSVI demonstrated a high R^2 value (>0.70) for both optical NDVI and ground biomass. Chang et al. (2018) developed the polarimetric radar vegetation index (PRVI) based on the degree of polarization of partially polarized waves, which exhibited a strong correlation with shrub biomass (R^2 = 0.75). Mandal et al. (2020b) utilized scattering information, including the degree of polarization and the eigenvalue spectrum, to derive the dual-pol radar vegetation index (DpRVI) from dual-pol SAR data. The linear regression model based on DpRVI accurately estimated biophysical parameters for three different crops.

The sensitivity of SAR parameters to crop height has been extensively studied (Erten et al., 2016). The key to this type of method is to establish relationships between radar features like backscatter coefficient and radar vegetation index, and crop height. This involves deriving expressions from observed data to determine the target parameters (McNairn and Shang, 2016). However, the combination of crop type, growing environment, and temporal dynamics adds complexity to crop monitoring. Models based on empirical statistics are challenging to apply in highly complex field environments. Firstly, plant height inversion requires ground-based observation experiments that are synchronized with satellite imaging. Models developed at specific points in time cannot account for changes in RVI responses caused by growth process differences. Secondly, models constructed from observational data have limitations and define the boundaries of the model. They are unable to accurately predict crop types with significant differences in population growth compared to the observed data populations.

In recent studies, researchers (Li et al., 2022b; Liu et al., 2023; Yang et al., 2022b; Zhao et al., 2022) have explored the

This contribution has been peer-reviewed. The double-blind peer-review was conducted on the basis of the full paper.
https://doi.org/10.5194/isprs-annals-X-1-2024-225-2024 | © Author(s) 2024. CC BY 4.0 License.

relationship between physiological parameters (such as aboveground biomass and plant area index) and vegetation indices during different growing seasons. They have developed models that capture the continuous relationship between discrete segmented vegetation indices and physiological parameters by parameterizing the vegetation indices, physiological parameters, and regression coefficients of specific crop canopies. A crucial assumption in this modeling approach is that the growth stages of crops can be digitized. Li et al. (2022b) have demonstrated that using phenological scales as continuous variables is highly effective for predicting model coefficients. While obtaining phenological scales through field surveys at the field scale is relatively straightforward, obtaining regular phenological information at the regional scale presents more challenges. The research idea of incorporating a temporal dimension to address the issue of estimating crop growing status is widely adopted in phenology estimation (Mascolo et al., 2021; McNairn et al., 2018; Silva-Perez et al., 2022; Yang et al., 2021), enabling the monitoring of crop growing status over multiple years. While other remote sensing studies are also employing this technique, further research is necessary to understand how to consider the dynamic context in plant height estimation.

The growth cycle of a crop involves changes in its structure, crop cover, and appearance, which in turn affect how it responds to vegetation indices. Previous studies (Kushwaha et al., 2022; Mandal et al., 2021; Nasirzadehdizaji et al., 2019) have shown that the SAR signal interacts more effectively with the entire crop structure during the pre-growth phase when there is less canopy cover. However, when the crop has a dense canopy cover, this interaction with the SAR signal is limited. Although the mechanisms behind this phenomenon are relatively simple, there is still a need for more research to identify specific vegetation structures that correspond to changes in the response of vegetation indices.

RVI has demonstrated good coherence in estimating plant height dynamics (Liu et al., 2023). Therefore, this study develops a dynamic model based on RVI for crop monitoring throughout the entire growing period. The objective is to investigate the impact of crop growth differences, including growth process differences and population growth differences, on the RVI response mechanism and plant height estimation. The research objectives are as follows: (1) Analyse the interrelationship between plant height and RVI at different fertility stages. (2) Assess the predictive performance of dynamic monitoring models throughout the entire growth period. (3) Explore and compare the vegetation structure of rice, wheat, and maize at the RVI saturation stage. (4) Discuss the factors influencing the differences in response to RVI among the three crops.

2. Materials and Methods

2.1 Study area

Field experimental data was collected from two provinces in China: Jiangsu and Shandong (Figure 1). The data included information on different crop rotation systems, growing seasons, varieties, and field management practices for rice, wheat, and maize crops. The types of crops grown varied across regions due to the differences in crop rotation systems among the study areas.

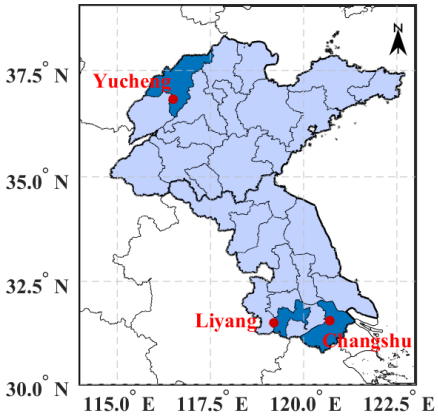

Figure 1. Geographical location of the study area.

2.2 Datasets

The data used in this study include: (a) Sentinel-1 IW Level 1 (L1) Ground Range Detected (GRD) products, which provide dual-polarization images of VV and VH; and (b) field data obtained from on-site surveys, including information on geographic location, crop types, crop height, and phenology.

We utilized Google Earth Engine (GEE) to obtain the backscatter coefficients for the study areas of Liyang, Changshu, and Yucheng. GEE officially preprocesses the GRD products (Gorelick et al., 2017), mainly by updating the orbital metadata with the orbital files; removing GRD boundary noise; removing thermal noise; radiometric calibration; and terrain correction (ortho-correction). The RVI proposed (Kim and Van Zyl, 2009) for quad-polarized SAR data, was modified for Sentinel-1 dual-pol data (VV and VH) as

$$RVI = 4\sigma^0_{vh}/(\sigma^0_{vv} + \sigma^0_{vh}) \quad (1)$$

Where σ^0_{vv}= the backscattering coefficient of co-polarization
σ^0_{vh}= the backscattering coefficient of cross-polarization

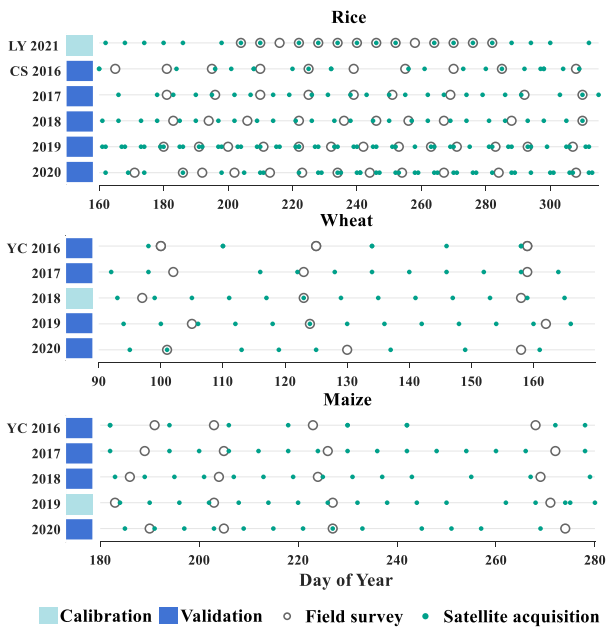

Figure 2. Data acquisition schedule for the study area.

This contribution has been peer-reviewed. The double-blind peer-review was conducted on the basis of the full paper.
https://doi.org/10.5194/isprs-annals-X-1-2024-225-2024 | © Author(s) 2024. CC BY 4.0 License.

Figure 2 summarizes the acquisition dates for each study area. The dates of field surveys or the Liyang region corresponded to the satellite image acquisition dates, suitable for training and validating samples for monitoring models. Field data from the Changshu and Yucheng regions between 2016 and 2020, were used as test samples to verify the height estimation. These historical data may not be synchronized with satellite data, requiring interpolation of observed values to obtain the best estimate of image acquisition dates.

To determine the natural plant height of the crops, we measure the vertical distance from the ground to the top of the main stem using a sampling method. The average value of these measurements represents the overall condition of the field. The phenological information of the crops is recorded using the BBCH scale. This scale assigns continuous numbers from 0 to 99 to describe the growth stages of crops (Lancashire et al., 1991), as shown in Table 1. It is worth noting that the BBCH code for maize is different from other crops as it lacks BBCH 20-29 and BBCH 40-49. To ensure the continuity of values, this study adjusted the BBCH Code for maize.

BBCH code	Rice	Wheat	Mazie	
			Before adjustment	After adjustment
00-09	Germination			-
10-19	Leaf development			-
20-29	Tillering		-	Germination
30-39	Stem elongation			Leaf development
40-49	Booting		-	Stem elongation
50-59	Inflorescence emergence, heading			
60-69	Flowering, anthesis			
70-79	Development of fruit			
80-89	Ripening			
90-99	Senescence			

Table 1. Phenological growth stages and BBCH code.

2.3 Conventional method for predicting PH

The conventional crop physiological parameters inversion research often uses single or segmented models to describe these relationships. In order to accurately describe the relationship between crop height and RVI at different growth stages, a least squares regression model based on different growth stages is constructed.

$$PH = k \times RVI + b \quad (2)$$

where k = the coefficient of the least squares regression model
b = the intercept of the least squares regression model

2.4 Development of dynamic monitoring model

Most models are developed and tested at specific time points, usually associated with a fixed phenological stage. Recent studies (Li et al., 2022b; Liu et al., 2023; Yang et al., 2022b; Zhao et al., 2022) have shown that models for different growth stages exhibit a changing relationship with increasing growth stages, specifically related to phenological advancement. The intercepts and coefficients within these models should also demonstrate a changing relationship with the stage of crop development.

$$k = \sum_{i=0}^{n} w'_i \times BBCH^i \quad (3)$$

$$b = \sum_{i=0}^{n} w''_i \times BBCH^i \quad (4)$$

where $BBCH$ = the crop phenological scale
n = the order of the polynomial
w'_i, w''_i = polynomial parameters

Through the use of polynomial continuous functions with specific forms described in (2), (3), and (4), it is possible to estimate PH during any phenological period.

$$PH = \sum_{i=0}^{n} (w'_i \times RVI + w''_i) \times BBCH^i \quad (5)$$

2.5 Interpolation of measured data

Despite the diverse growing conditions, crops generally exhibit a consistent growth pattern. Growth curves offer valuable insights into the expected values of crop biophysical parameters at each growth stage, aiding in the determination of adaptive parameters (Marinakis, 2012; Yoshimoto, 2001). The Richards growth equation was employed to simulate the curve of plant height. The equation's basic form is as follows

$$PH = a/(1 + e^{b-c*BBCH})^{1/d} \quad (7)$$

where a = the maximum plant height value
b = the initial value parameter
c = the growth rate parameter
d = the curve trait parameter

2.6 Shape model fitting

In this study, shape model fitting method (Liu et al. 2022; Sakamoto 2018) was used to suitably adjust and optimize (3) and (4) for different crops. The method uses a preliminarily defined time series shape model $g(x)$ to match the time series (3) and (4) based on linear offset and scaling steps, which are represented as

$$\hat{g}(x) = yscale \times \left[g\left(xscale \times (x + tshift)\right) + bias\right] + bias \quad (8)$$

where $g(x)$ = the preliminarily defined shape models
$\hat{g}(x)$ = geometrically transformed from $g(x)$
$xscale$ = the scaling parameters in x directions
$yscale$ = the scaling parameters in y directions
$tshift$= displacement parameter
$bias$ = the value fixed for each crop species

3. Results and Discussion

3.1 Impact of growth process differences on conventional method

Dense time series data help distinguish different crop growth stages. In this subsection, we took rice as an example and selected data from the Liyang area in 2021, focusing on different growth stages for comparison. Figure 3 shows the temporal dynamics of crop height, temporal variations of RVI, the relationship between RVI and PH at different phenological periods, and the temporal variations of model parameters, respectively.

Figure 3 (a) shows the variation in the measured PH and rice growth rate with the phenological scale. Before the maturity period, the crop had grown rapidly, and the PH had continually increased. During the maturity period, the plant stopped growing, and the PH fluctuated within a small range. RVI showed good sensitivity in early rice growth stages. However, the temporal curves were not monotonically increasing or decreasing. In addition, RVI saturated prematurely before plant height growth stopped. Therefore, it was difficult to directly identify the response of RVI to PH and to estimate PH using simple methods. Further analysis of rice data is needed.

Conventional regression method is commonly used to estimate crop biophysical parameters due to their simplicity. However, these methods often overlook the phenological variations of crops. The scatter plots between PH and RVI indicate a strong relationship at all stages. However, there is no consistent mapping from RVI to PH throughout the entire growing season. The regression model developed for a specific phenological period is effective only for a single time phase or a portion of the rice growth cycle, which introduces errors in PH estimation. For instance, when RVI = 1, it may correspond to multiple PHs in different phenological periods. Figure 3 (d) illustrates the time-series relationship of the linear VI-PH model parameters, specifically the slope and intercept. The introduction of a time dimension may help to address the dynamics of the model parameters, which is a commonly used approach in other remote sensing fields.

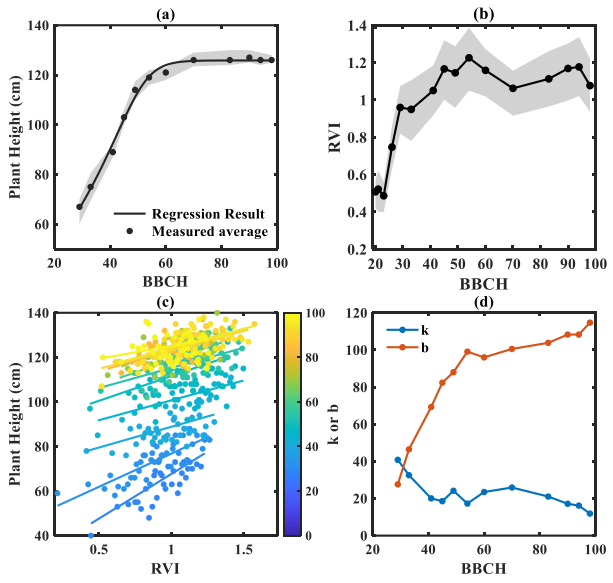

Figure 3. (a) Temporal dynamics of crop height. (b) Temporal variation of RVI. (c) The relationship between RVI and PH at different phenological periods. (d) Temporal variations of model parameters. The positions of the upper and lower ends of the light region correspond to the upper and lower quartiles (Q3 and Q1) of the inverted plant height.

3.2 Predictive performance of dynamic monitoring models

This study calibrates the dynamic monitoring models for the three crops using 2021 rice data, 2018 wheat data and 2019 maize data, respectively. Building on previous research, this study adopts a 5th-order polynomial for fitting. The limited amount of actual measurement data in the Yucheng region may result in poor performance of the model in other phenological stages. This study uses simulated plant height values to calibrate dynamic monitoring models for wheat and maize. The fitting results are illustrated in Figure 4. To enhance the accuracy of the dynamic monitoring model for maize, we have individually processed and adjusted BBCH 42-48 during the calibration process.

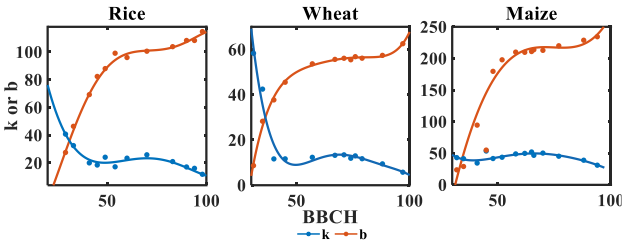

Figure 4. k and b fitting results for the three crops.

In Figure 5, the estimated plant height values of dynamic monitoring models are compared with the ground truth data. In general, plant height inversion accuracy was highest for wheat (R^2 = 0.8799, RMSE = 5.6667 cm, MAPE = 8.5172 %) and poorer for rice (R^2 = 0.2742, RMSE = 17.2895 cm, MAPE = 18.1418 %) and maize (R^2 = 0.9720, RMSE = 16.5877 cm, MAPE = 14.1513 %). Although the accuracy of the inversion varies among the three crops, they all exhibit a similar pattern. Specifically, the plant height monitoring results maintain a high accuracy within a certain height range. However, once this threshold is surpassed, the accuracy gradually declines. The height thresholds for the respective crops are indicated by red dashed lines in the accuracy plot. For rice, the threshold is 75 cm, for wheat it is 52 cm, and for maize it is 150 cm. We attribute this phenomenon to the limitations of SAR penetration and premature saturation of RVI caused by the attenuation effect as the crop plant grows taller and denser.

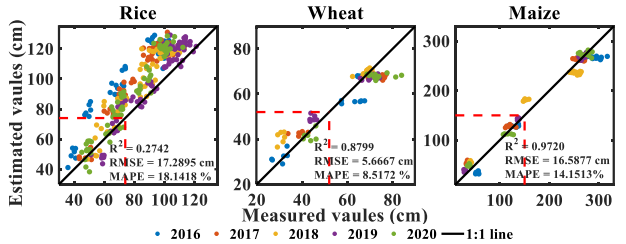

Figure 5. Inversion accuracy of plant height for rice, wheat and maize.

Considering the asynchrony between field measurements and remote sensing data, the temporal inversion results of the model are compared to the regression results of ground truth values in Figure 6 The inversion plant height curves showed a consistent trend with the observed plant height curves. However, the estimation errors gradually increased as the growth differences between crops became more evident, particularly in rice and maize. In terms of crop growth stage, the three crops had the highest accuracy in most cases before the jointing or mid-jointing stage. From the tillering stage onwards, the plants develop distinct vertical structures and interact well with SAR signals, leading to a steady increase in RVI. As the height of the plants and the density of the leaves reach a certain level, the surface of the rice area becomes uniform and dense. This uniformity and density limit the penetration and reflection of SAR signals, resulting in the RVI approaching saturation and maintaining relative stability. Previous studies have also confirmed that during the early vegetation stage of crops, specifically between the tillering and booting stages, the sensitivity of Sentinel-1 backscattering coefficients to crop biophysical parameters is the highest.

This contribution has been peer-reviewed. The double-blind peer-review was conducted on the basis of the full paper.
https://doi.org/10.5194/isprs-annals-X-1-2024-225-2024 | © Author(s) 2024. CC BY 4.0 License.

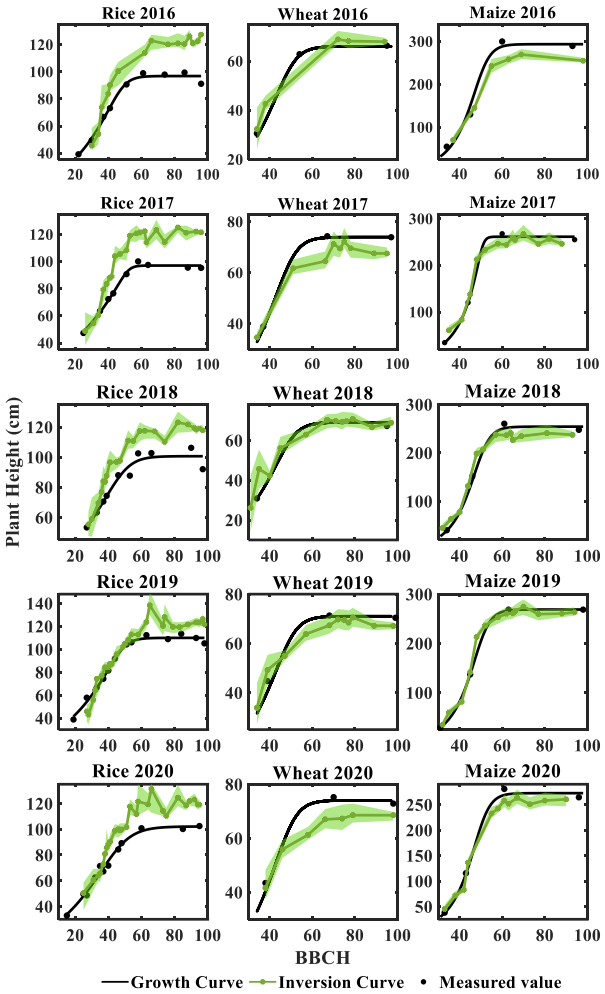

Figure 6. Comparison between the retrieved plant height and the ground truth values. The positions at the upper and lower ends of the light green area correspond to the upper and lower quartiles (Q3 and Q1) of the retrieved plant height.

3.3 Impact of population growth differences on dynamic monitoring models

The maximum plant height of crop growth can vary significantly due to the influence of growth environment and crop species. Figure 7 illustrates the correlation between the difference in maximum crop height and the RMSE between the calibration and validation datasets. The analyses showed that the greater the growth differences between crops, the worse the plant height estimates. The disparities in crop growth between the calibration dataset and the validation dataset are significant factors influencing the accuracy of plant height monitoring. Therefore, models developed exclusively for specific spatial scales and crop varieties cannot accurately and promptly predict crop growth in other regions or varieties.

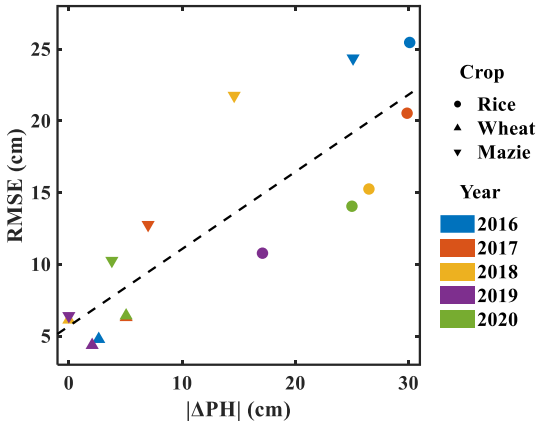

Figure 7. Statistical analysis of crop growth differences and precision of plant height estimation.

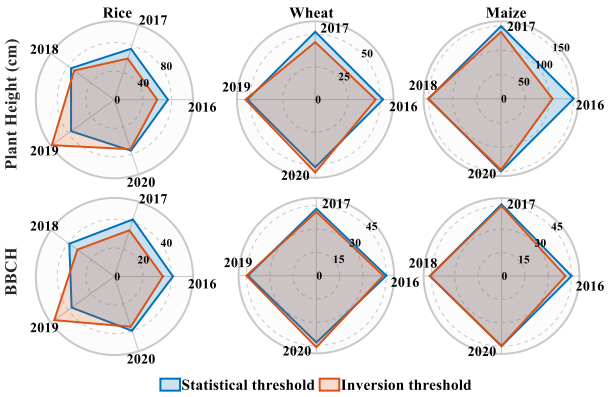

Figure 8. Comparison of statistical and inverse plant height thresholds and their corresponding phenological periods.

As shown in Figure 6, these models maintain precision until a certain period, even though differences in crop populations affect the accuracy of models. This discrepancy arises because RVI reaches saturation earlier than PH in different crop linear RVI-PH relationships. To provide further clarification on the crop growth conditions and corresponding phenological nodes for RVI saturation, Figure 8 displays the plant heights at which the inverse growth curves of the test set began to deviate from the measured growth curves. It also shows the corresponding phenological periods and compares them with the statistical thresholds of plant heights and their respective phenological periods for each year. In the case of rice, most of the plant heights at which the inverse growth curves deviated from the measured growth curves were either less than or close to the statistical threshold of 75 cm. These deviations mainly occurred during the pre- or mid-jointing stage, with only the monitoring results in 2019 performing well at the heading stage. For wheat and maize, the inversion structure exhibited fine agreement with the statistical threshold. Wheat reached RVI saturation at the pre-booting stage, while maize reached saturation at the pre-jointing stage. Previous studies by Kushwaha et al. (2022) found that the SAR signal exhibited the strongest correlation with plant height during the BBCH 21-49 stages of rice, with estimated values ranging from 40-80 cm. Similarly, Nasirzadehdizaji et al. (2019) and Liao et al. (2018) discovered through correlation analysis that the optimal wheat height is below 53 cm and the sensitivity of SAR parameters begins to decline when maize height exceeds 150 cm. These findings are consistent with our experimental results, although further research is necessary to investigate the

reasons for the differences in SAR parameter sensitivity to plant height among the three crops.

3.4 Differences in the effects of the three crops on RVI response

Rice, wheat, and maize are distinct crop types that differ in leaf sizes, orientations, and canopy structures. Leaf Area Index (LAI), which measures the area covered by vegetative leaves per unit of land surface, is a crucial vegetation parameter that characterizes leaf sparsity and canopy structure. It also plays a significant role in influencing the response of RVI. Additionally, planting density may limit SAR penetration capacity. Therefore, Figure 9 presents statistical data on the LAI and planting density corresponding to the inversion plant height threshold for crop vegetation structure.

The LAI values corresponding to plant height thresholds in different years were not concentrated within a specific range. For rice, the planting density was 25 plants or holes/m^2 from 2016 to 2020, and the corresponding LAI varied greatly at the similar plant height level. Hence, LAI may not be the primary cause of premature saturation of RVI. Maize, being a broadleaf crop, has a sparse planting density (averaging 6 plants or holes/m^2), resulting in a plant height threshold of approximately 150 cm. In comparison, wheat plants are densely planted (averaging 580 plants or holes/m^2), causing wheat to reach the inversion threshold earlier at the same LAI level. Therefore, planting density may be the primary factor limiting the vegetation structure characterized by RVI.

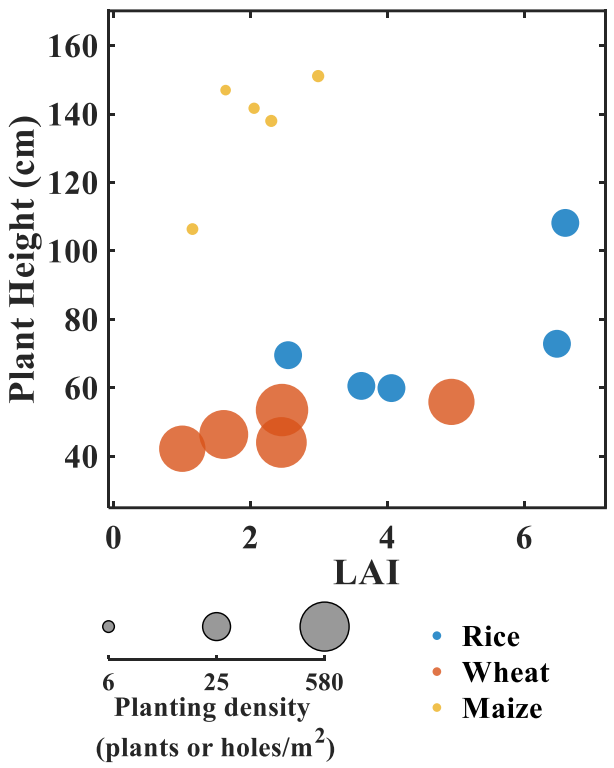

Figure 9. Statistics on LAI and planting density corresponding to inverse thresholds of plant height.

3.5 Study Limitations and future direction

The dynamic monitoring model addresses the limitations of traditional agricultural remote sensing models, which only work effectively on a single time phase or part of the growth cycle. It allows us to analyse the RVI response from the perspective of crop growth differences. However, the model itself has some limitations. Firstly, the fitting error of the model may result in outliers in plant height estimation during certain growth cycles, which can affect the determination of the plant height threshold. Future research could explore the use of machine learning or deep learning methods to solve this nonlinear problem and develop a more accurate plant height estimation model. Secondly, the model requires crop phenology information as input, which is typically characterized by BBCH and needs to be confirmed through field surveys. However, different observers may record BBCH differently, which can affect the assessment of growth differences in response to RVI. An alternative solution could be to use growing degree days (GDD) instead of BBCH to characterize crop growth stages (Li et al., 2022b; Yang et al., 2022b).

In terms of vegetation indices, this study primarily focuses on assessing the limitations of RVI for crop monitoring. However, other SAR parameters such as DPSVI, PRVI, and DpRVI, which have shown high correlation with crop biophysical parameters, need to be further discussed. Additionally, this study collected relatively few crop data and did not consider the effects of leaf scale and soil background on RVI saturation. Therefore, it is important to include datasets for more crop varieties or types and consider these factors in future research.

4. Conclusion

RVI has been extensively utilized for qualitative and quantitative remote sensing monitoring of vegetation growth dynamics. However, the phenomenon of premature saturation of RVI imposes limitations on its ability to characterize surface vegetation over dense vegetation canopy structures. Despite the relatively simple underlying mechanisms of this phenomenon, there is currently a lack of specific metrics to quantify the effect of vegetation structure on RVI. Building upon this premise, this study utilized a dynamic growth model to conduct dynamic monitoring of plant height for three common crops: rice, wheat, and maize. Furthermore, the study explores the limitations of RVI in accurately determining crop height. The experimental findings are summarized as follows:

(1) Models developed for specific spatial and temporal scales of particular crop varieties may not accurately predict crop growth in different regions or with different varieties in a timely manner, due to growth differences.

(2) These models maintain accuracy over a range of plant heights, such as rice at around 70cm, wheat at around 50cm, and maize at around 150cm.

(3) Among the three crops, planting density was identified as the main factor influencing the differences in RVI response.

Overall, traditional monitoring models face challenges in being widely applicable in highly complex field environments due to growth differences. However, the RVI demonstrates a strong correlation during the pre-growth period of crops, which can enhance our understanding of how radar signals respond to vegetation structure and planting techniques. The results of this study will contribute to integrating agronomic knowledge with spatio-temporal remote sensing data, and serve as a reference for the development of quantitative remote sensing models for smart agriculture.

Acknowledgements

This work was supported by Theory and Method of Satellite Dynamic Photogrammetry for Near-earth Space Object from the National Natural Science Foundation of China (NO. 42271448). Thanks to the in-situ data in Liyang observed by National Space Infrastructure Common Application Support Platform Nanjing Remote Sensing Authenticity Inspection Station. Dataset in Changshu and Yucheng is provided by National Ecosystem Science Data Center, National Science & Technology Infrastructure of China. Special thanks to the in-situ observation data from Changshu National Agricultural Ecosystem Observation Research Station affiliated with the Institute of Soil Science, Chinese Academy of Sciences, and Yucheng National Agricultural Ecosystem Observation Research Station.

References

Blaes, X., Defourny, P., Wegmuller, U., Della Vecchia, A., Guerriero, L., & Ferrazzoli, P., 2006. C-band polarimetric indexes for maize monitoring based on a validated radiative transfer model. *IEEE Transactions on Geoscience and Remote Sensing, 44*, 791-800

Chang, A., Jung, J., Maeda, M.M., & Landivar, J., 2017. Crop height monitoring with digital imagery from Unmanned Aerial System (UAS). *Computers and Electronics in Agriculture, 141*, 232-237

Chang, J.G., Shoshany, M., & Oh, Y., 2018. Polarimetric radar vegetation index for biomass estimation in desert fringe ecosystems. *IEEE Transactions on Geoscience and Remote Sensing, 56*, 7102-7108

Erten, E., Lopez-Sanchez, J.M., Yuzugullu, O., & Hajnsek, I., 2016. Retrieval of agricultural crop height from space: A comparison of SAR techniques. *Remote sensing of Environment, 187*, 130-144

Gorelick, N., Hancher, M., Dixon, M., Ilyushchenko, S., Thau, D., & Moore, R., 2017. Google Earth Engine: Planetary-scale geospatial analysis for everyone. *Remote sensing of Environment, 202*, 18-27

Kim, Y., & Van Zyl, J.J., 2009. A time-series approach to estimate soil moisture using polarimetric radar data. *IEEE Transactions on Geoscience and Remote Sensing, 47*, 2519-2527

Kushwaha, A., Dave, R., Kumar, G., Saha, K., & Khan, A., 2022. Assessment of rice crop biophysical parameters using Sentinel-1 C-band SAR data. *Advances in Space Research, 70*, 3833-3844

Lancashire, P.D., Bleiholder, H., Boom, T.V.D., Langelüddeke, P., Stauss, R., Weber, E., & Witzenberger, A., 1991. A uniform decimal code for growth stages of crops and weeds. *Annals of applied Biology, 119*, 561-601

Li, Z., Zhao, Y., Taylor, J., Gaulton, R., Jin, X., Song, X., Li, Z., Meng, Y., Chen, P., & Feng, H., 2022b. Comparison and transferability of thermal, temporal and phenological-based in-season predictions of above-ground biomass in wheat crops from proximal crop reflectance data. *Remote sensing of Environment, 273*, 112967

Liao, C., Wang, J., Shang, J., Huang, X., Liu, J., & Huffman, T., 2018. Sensitivity study of Radarsat-2 polarimetric SAR to crop height and fractional vegetation cover of corn and wheat. *International Journal of remote sensing, 39*, 1475-1490

Liu, L., Cao, R., Chen, J., Shen, M., Wang, S., Zhou, J., & He, B., 2022. Detecting crop phenology from vegetation index time-series data by improved shape model fitting in each phenological stage. *Remote sensing of Environment, 277*, 113060

Liu, Y., Wang, B., Sheng, Q., Li, J., Zhao, H., Wang, S., Liu, X., & He, H., 2023. Dual-polarization SAR rice growth model: A modeling approach for monitoring plant height by combining crop growth patterns with spatiotemporal SAR data. *Computers and Electronics in Agriculture, 215*, 108358

Mandal, D., Bhattacharya, A., & Rao, Y.S., 2021. *Radar remote sensing for crop biophysical parameter estimation*. Springer

Mandal, D., Kumar, V., Ratha, D., Dey, S., Bhattacharya, A., Lopez-Sanchez, J.M., McNairn, H., & Rao, Y.S., 2020b. Dual polarimetric radar vegetation index for crop growth monitoring using sentinel-1 SAR data. *Remote sensing of Environment, 247*, 111954

Marinakis, Y.D., 2012. Forecasting technology diffusion with the Richards model. *Technological Forecasting and Social Change, 79*, 172-179

Mascolo, L., Martinez-Marin, T., & Lopez-Sanchez, J.M., 2021. Optimal grid-based filtering for crop phenology estimation with sentinel-1 SAR data. *Remote Sensing, 13*, 4332

McNairn, H., Jiao, X., Pacheco, A., Sinha, A., Tan, W., & Li, Y., 2018. Estimating canola phenology using synthetic aperture radar. *Remote sensing of Environment, 219*, 196-205

McNairn, H., & Shang, J., 2016. A review of multitemporal synthetic aperture radar (SAR) for crop monitoring. *Multitemporal Remote Sensing: Methods and Applications*, 317-340

Nasirzadehdizaji, R., Balik Sanli, F., Abdikan, S., Cakir, Z., Sekertekin, A., & Ustuner, M., 2019. Sensitivity analysis of multi-temporal Sentinel-1 SAR parameters to crop height and canopy coverage. *Applied Sciences, 9*, 655

Pang, J., Zhang, R., Yu, B., Liao, M., Lv, J., Xie, L., Li, S., & Zhan, J., 2021. Pixel-level rice planting information monitoring in Fujin City based on time-series SAR imagery. *International Journal of Applied Earth Observation and Geoinformation, 104*, 102551

Periasamy, S., 2018. Significance of dual polarimetric synthetic aperture radar in biomass retrieval: An attempt on Sentinel-1. *Remote Sensing of Environment, 217*, 537-549

Sakamoto, T., 2018. Refined shape model fitting methods for detecting various types of phenological information on major US crops. *ISPRS Journal of Photogrammetry and Remote Sensing, 138*, 176-192

Silva-Perez, C., Marino, A., & Cameron, I., 2022. Learning-based tracking of crop biophysical variables and key dates estimation from fusion of SAR and optical data. *IEEE Journal of Selected Topics in Applied Earth Observations and Remote Sensing, 15*, 7444-7457

Steele-Dunne, S.C., McNairn, H., Monsivais-Huertero, A., Judge, J., Liu, P.-W., & Papathanassiou, K., 2017. Radar remote sensing of agricultural canopies: A review. *IEEE Journal of Selected Topics in Applied Earth Observations and Remote Sensing, 10*, 2249-2273

Veloso, A., Mermoz, S., Bouvet, A., Le Toan, T., Planells, M., Dejoux, J.-F., & Ceschia, E., 2017. Understanding the temporal behavior of crops using Sentinel-1 and Sentinel-2-like data for agricultural applications. *Remote Sensing of Environment, 199*, 415-426

Weiss, M., Jacob, F., & Duveiller, G., 2020. Remote sensing for agricultural applications: A meta-review. *Remote sensing of Environment, 236*, 111402

Wu, B., Zhang, M., Zeng, H., Tian, F., Potgieter, A.B., Qin, X., Yan, N., Chang, S., Zhao, Y., & Dong, Q., 2023. Challenges and opportunities in remote sensing-based crop monitoring: a review. *National Science Review, 10*, nwac290

Yang, H., Pan, B., Li, N., Wang, W., Zhang, J., & Zhang, X., 2021. A systematic method for spatio-temporal phenology estimation of paddy rice using time series Sentinel-1 images. *Remote sensing of Environment, 259*, 112394

Yang, Q., Shi, L., Han, J., Chen, Z., & Yu, J., 2022b. A VI-based phenology adaptation approach for rice crop monitoring using UAV multispectral images. *Field Crops Research, 277*, 108419

Yoshimoto, A., 2001. Application of the Logistic, Gompertz, and Richards growth functions to Gentan probability analysis. *Journal of forest research, 6*, 265-272

Zhao, Y., Meng, Y., Han, S., Feng, H., Yang, G., & Li, Z., 2022. Should phenological information be applied to predict agronomic traits across growth stages of winter wheat? *The Crop Journal, 10*, 1346-1352